International Journal of Manufacturing Economics and Management
ISSN 2784-1278 ISSN-L 2784-1278, Vol. V, No. 2 / 2025
https://doi.org/10.54684/ijmem.2025.5.2.25

MECHANICAL DESIGN AND FABRICATION OF A PROTOTYPE BALLBOT SYSTEM

Tran Vu Minh[1] , Nguyen Xuan Quynh[1], Nguyen Thi Anh[2], Tran Thanh Tung[3]

School of Mechanical Engineering, Ha Noi University of Science and Technology, Ha Noi, Vietnam[1]
Faculty of Mechanical Engineering, Thuyloi University, Vietnam[2]
Faculty of Engineering Mechanics and Automation, University of Engineering and Technology, Vietnam National University, Hanoi, Vietnam [3]

Corresponding author: Tran Thanh Tung, tranthanhtung@vnu.edu.vn

Abstract: This paper presents the mechanical design, fabrication, and performance evaluation of a BallBot, a self-balancing mobile robot that moves on a single spherical ball. The objective is to develop a compact, stable, and omnidirectional platform capable of carrying a 50 N payload while maintaining dynamic stability on both flat and inclined surfaces. The robot is driven by three omni-wheel motor modules, each mounted at a 45° angle to the ball's surface, enabling precise motion control. A novel support frame with an integrated spring damping mechanism ensures consistent ball contact and reduces structural vibrations. Additionally, a spring-based ball return system with roller-assisted contact reduces friction and improves positional accuracy during movement. Experimental results indicate that while the BallBot achieves a velocity of ~0.49 m/s under no load, performance degrades significantly under higher payloads, with complete mobility loss beyond 30 N. The findings highlight the design's effectiveness under light loads and suggest further improvements in torque output and control strategies for enhanced load-carrying capabilities.

Keywords: mechanical, design, ballbot, mobile robot

1. INTRODUCTION

In recent years, advancements in robotics have led to the emergence of novel mobile platforms that offer enhanced agility, compactness, and versatility [1-8]. Among these, the BallBot stands out as a unique robotic system capable of balancing and maneuvering atop a single spherical ball [9-15]. This configuration allows for omnidirectional movement in tight spaces without the need to reorient the robot's body, making it an ideal solution for navigation in constrained or dynamic environments.

The BallBot's mechanical design presents a distinct set of engineering challenges. Unlike conventional wheeled robots, BallBot requires a precisely balanced and symmetrical structure, as well as a mechanically robust support system capable of maintaining stability on a constantly moving spherical surface [16-20]. The core of the system consists of a multi-tiered robot frame mounted above a ball, with motion generated through the coordinated actuation of three omni wheels, each driven by an individual motor and positioned at 45° relative to the horizontal plane. This geometric arrangement must be carefully designed to ensure optimal contact with the ball, efficient transmission of driving force, and minimal structural vibration.

To meet these demands, this project focuses on the mechanical design and fabrication of a BallBot prototype, including critical subsystems such as the motor mount assembly, support frame, spring-damped base, and a ball return mechanism. Emphasis is placed on achieving a balance between structural rigidity, weight distribution, manufacturability, and modularity. Special attention is given to minimizing friction at the ball contact points, ensuring precise alignment of components, and enabling mechanical adjustability to improve reliability under varying loads and surfaces.

By addressing these mechanical aspects in depth, the study aims to lay a solid foundation for future developments in control algorithm integration, sensor fusion, and real-world deployment. The resulting BallBot platform not only demonstrates innovative mechanical engineering but also serves as a versatile testbed for further research in autonomous balancing robotics.

2. DESIGN REQUIREMENTS AND SYSTEM OVERVIEW

2.1. Design objectives

The objective is to design and fabricate a BallBot model capable of traversing a flat surface and an inclined plane at an inclination of less than 20 degrees, while carrying a weight of less than 50N. The Robot's structural system comprises a sphere with a diameter of 240 mm, and the total height of the Robot's frame is 600 mm, as illustrated in Figure 1.

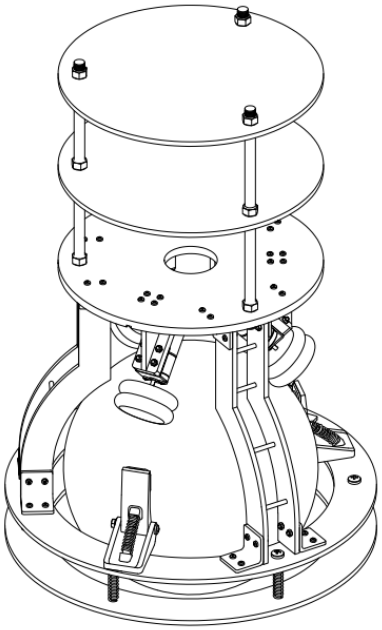

Fig. 1. Initial BallBot prototype model

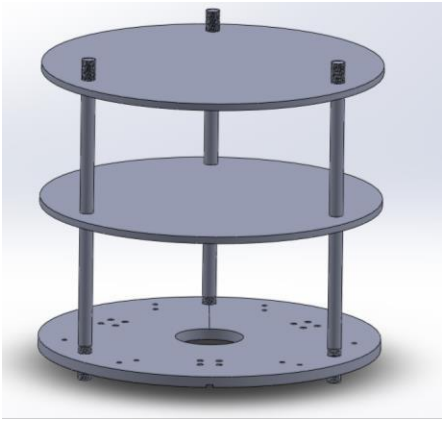

Fig. 2. Ballbot frame

Figure 2 describes the structure of the robot frame, consisting of 3 floors: the first floor (base) is designed to be assembled with connecting legs, the second floor is where the control devices, batteries, sensors, etc. are arranged, and the third floor is designed to place heavy objects.

2.2. Mechanical Design

2.2.1. Motor Mount Design

Design Requirements and Functional Considerations: The motor mount is a critical intermediate component in the BallBot system, serving to mechanically connect the drive motor to both the omni-wheel and the upper structural frame. The mount must satisfy several essential functional requirements to ensure reliable system performance. First, the design must precisely maintain a 45-degree tilt angle between the motor axis and the bottom reference plane. This orientation ensures that the contact interface between the omni-wheel and the surface of the spherical ball is tangential, which is necessary for efficient and stable motion transmission. Second, the mount must provide a rigid and mechanically robust structure capable of supporting an external static load of 50 N, representing the downward force from the upper frame and any onboard components. This load-bearing requirement was addressed through the inclusion of reinforcement ribs in the final design, as well as optimized material thicknesses to resist bending and shear stresses. Furthermore, precise alignment features were integrated into the design to maintain the integrity of the 45-degree mounting angle during both fabrication and assembly. The final geometry thus balances spatial constraints, manufacturability, and mechanical performance, ensuring the motor operates at the correct orientation while maintaining structural stability under loading.

The design of the engine mount, as shown in Figure 3, introduces several enhancements over the initial concept to improve mechanical strength and stability. Most notably, structural reinforcement ribs have been added along the inclined face. These ribs significantly increase the mount’s stiffness, particularly under dynamic loading conditions such as torque fluctuations or vibrations from motor operation. The upper surface retains bolt holes to ensure secure fastening to the chassis, maintaining compatibility with the modular frame design. The geometry of the bracket remains compact and optimized for manufacturing, while the additional ribs reduce flexing and extend the fatigue life of the mount under repeated use. These modifications were made in response to preliminary testing, which indicated slight deformation in the original mount during motor acceleration. The final design, therefore, balances material usage, manufacturability (via 3D printing or machining), and mechanical robustness, making it well-suited for integration into the BallBot's spherical drive system.

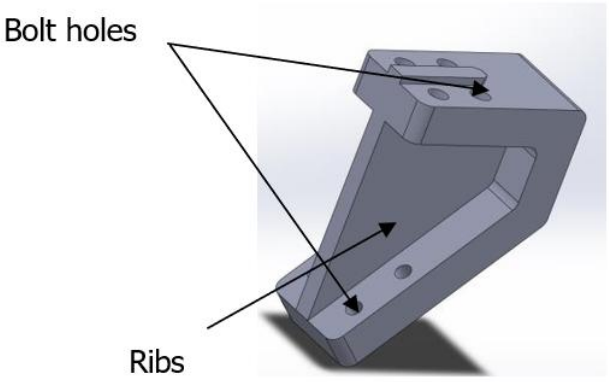

Fig. 3. The design of the engine motor mount

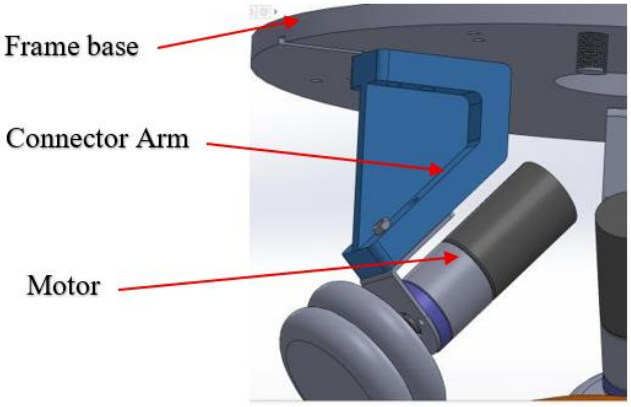

Fig. 4. Mounting Position of the Motor Assembly

Figure 4 above illustrates the mounting configuration of the motor assembly in the BallBot system, highlighting the integration between the connector bracket, motor, and the upper structural frame. The connector arm, which corresponds to the previously optimized motor mount, is rigidly fastened to the bottom surface of the top plate via pre-drilled bolt holes. This mounting configuration establishes a fixed 45-degree tilt angle between the motor axis and the horizontal plane, aligning the omni-wheel tangentially with the surface of the spherical ball. Such an orientation is critical for ensuring efficient and stable force transfer from the motor to the ball during omnidirectional movement. The bracket's geometry, including reinforcement ribs and precise bolt positioning, is specifically designed to maintain this alignment under both static and dynamic loading. Additionally, the overall layout minimizes spatial interference with neighboring components, allowing a symmetrical and balanced distribution of multiple motor assemblies around the BallBot's lower shell.

2.2.2. Design of support frame

The support frame is engineered to encase the BallBot's spherical drive unit with a clearance of approximately 15–20 mm, allowing sufficient freedom for the ball to rotate in all directions while ensuring protection and structural stability. A circular base ring surrounds the ball near ground level, serving both as a space-saving constraint and a weight-distribution mechanism, effectively lowering the BallBot's center of gravity. This configuration significantly enhances the robot's dynamic stability during operation by keeping the center of mass below the upper chassis. Additionally, the external frame provides a protective barrier for sensitive components mounted on the robot, reducing the risk of damage during assembly, testing, and operation.

The support structure is mechanically connected to the base of the main chassis through three equally spaced connecting bars, arranged at 120-degree intervals. These bars are custom-designed to match the curvature and diameter of the spherical ball, ensuring a secure fit and maintaining overall alignment. The material selected for the frame is mica-coated steel, which offers a good balance between mechanical strength and machinability. The individual bars are assembled using M4 bolts and nuts, with Ø5×20 mm hollow spacers inserted between the joints to maintain precise inter-bar spacing as per the design specification. This modular approach enables ease of manufacturing, assembly, and disassembly, while preserving the structural integrity required for reliable BallBot performance.

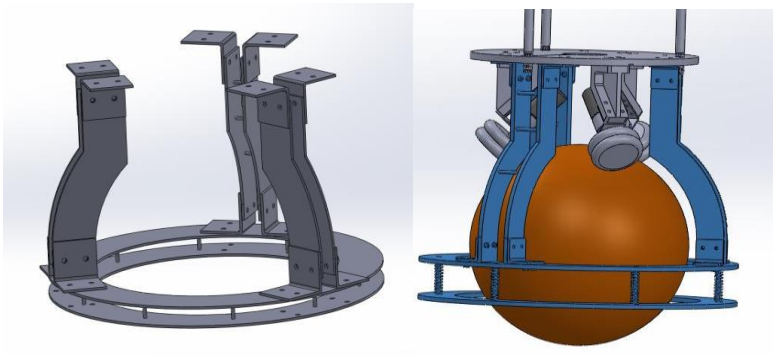

Fig. 5. Support Frame Design

The support frame forms the structural backbone of the BallBot and is responsible for maintaining mechanical integrity, precise alignment of components, and protecting the internal spherical drive mechanism. As shown in Figure 5, the frame consists of curved vertical struts attached to both a top circular mounting plate and a lower stabilizing ring. These struts are symmetrically distributed to provide balanced load support while allowing sufficient clearance for the spherical ball housed within the structure. The assembled configuration, shown on the right, demonstrates how the omni-wheel motor modules are mounted at a 45-degree angle toward the ball's surface using precision engineered brackets. The frame's open design ensures minimal weight while preserving rigidity, and its circular footprint accommodates uniform force distribution during omnidirectional motion. This modular frame can be fabricated using laser-cut aluminum or acrylic sheets fastened with screws, facilitating ease of assembly, maintenance, and future modifications.

To reduce friction during movement, a roller system (Figure 6) was integrated into the support structure. This system includes six evenly spaced rollers at 60° intervals around a ring-shaped frame, allowing the robot's load to be distributed evenly for smoother operation.

However, during the design phase, it was found that the distance from the main frame base to the ground was sensitive to variations in ball surface tension, causing misalignment between the motor and ball, and leading to improper contact of the omni-wheels. These deviations, if repeated, reduced the system's stability and contradicted the original design calculations.

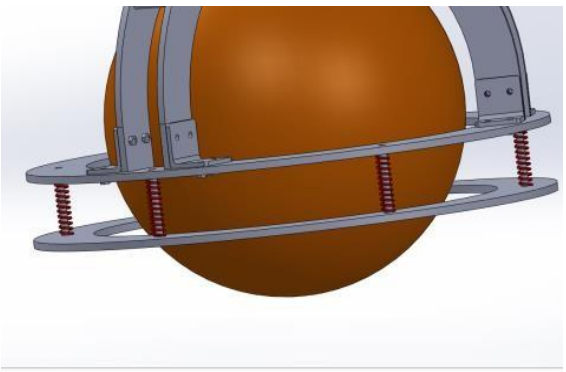

Fig. 6. Bolt-Spring Alignment Unit

To address this, a spring system was added beneath the support frame. This addition allows adjustment of the frame height, improving contact consistency and enabling the BallBot to operate more reliably, even on slightly uneven surfaces. The final optimized support design is illustrated in Figure 6

Spring Stiffness Calculation and Installation Adjustment

To ensure proper load distribution and ground contact for the support system, a spring-based damping mechanism was incorporated beneath the support frame. The design requires the system to support a total load of 5 kg, distributed equally across six springs, with a maximum allowable compression (displacement) of 10–15 mm.

The force acting on each spring is calculated as:

$$F=\frac{P}{n}=8.33\ \text{N} \quad (1)$$

Using Hooke's Law, the required spring stiffness KKK is:

$$K=\frac{F}{\Delta x}=555.5\ \text{N/m} \quad (2)$$

A spring length of 30–35 mm is selected to provide sufficient preload and installation tolerance. During assembly, the mounting bolts are adjusted to ensure that the support structure makes uniform contact with the ground, helping to stabilize the system and prevent uneven wheel contact. This configuration improves overall performance and helps the BallBot operate more stably across variable surfaces.
Start by choosing a spring index C= D/d; a typical, manufacturable spring index is C= 8.
For a round wire helical compression spring:

$$k = \frac{Gd^4}{8D^3N} \quad (3)$$

where: G= 80. 10^9 Pa, d= 1mm and then N= 3.55.

Shear stress in spring is:

$$\tau = \frac{8FDK}{\pi d^3} \quad (4)$$

where: $K = \frac{4C-1}{4C-4} + \frac{0.615}{C}$

For C=8, K =1.25, and then τ = 208 MPa.
The selected spring is designed to meet both the static load and dynamic operational requirements of the BallBot's support system. With a calculated stiffness of 550 N/m, a wire diameter of 1.0 mm, and a mean coil diameter of 8.0 mm, the resulting maximum shear stress under full compression is approximately 208 MPa, which is well below the typical endurance limit for music wire (≈ 340–400 MPa in fatigue for repeated loading). This ensures the spring operates safely within the elastic range and does not approach yielding or fatigue failure under normal conditions. The spring features a spring index (C) of 8, which balances manufacturability and stress concentration, contributing to long service life. In addition, the number of working coils (≈3.5) and moderate deflection (15 mm) minimize stress fluctuations during repeated compressions, improving fatigue resistance. Overall, the spring design provides adequate strength, elasticity, and durability for continuous operation in the robot's support system.

2.2.3. Ball Return System Design

The BallBot achieves balance and motion through the coordinated control of its three omni-wheels. However, due to the nature of omni-wheel mechanics, the resultant forces applied to the ball are not always symmetric or self-canceling. During certain maneuvers or uneven weight distribution, the forces transmitted from the wheels can cause the ball to deviate from its ideal central position. This displacement results in undesired shifts in the robot's center of mass, potentially leading to operational instability or inaccurate response from the control system.
To mitigate this issue, the design team implemented a passive ball return mechanism, consisting of three spring-loaded return units evenly distributed at 120-degree intervals along the lower support frame (as shown in Figure 7). These units exert a gentle, centering force on the ball whenever it deviates from the neutral position, ensuring that the ball naturally returns to its calibrated center when external driving forces are reduced. The spring tension is carefully selected to be strong enough to correct positional drift without interfering with the robot's dynamic balancing functions. This addition improves the operational stability, repeatability, and responsiveness of the BallBot during both movement and idle states.
The ball return system operates based on the elastic restoring force of compression springs, which are used to reposition the ball to its neutral center. The design includes three identical return units, each consisting of a spring, a base, and a push plate. These units are symmetrically positioned at 120-degree intervals around the lower perimeter of the support frame, ensuring uniform force application. When the ball deviates from its central position due to uneven forces from the omni-wheels, the push plates apply a restoring force directed along the vertical axis of the ball. This configuration ensures that the restoring forces are balanced and radially symmetric, helping the ball return to its optimal central position without interfering with its intended motion. As a result, the system improves the positional accuracy and stability of the BallBot, particularly during transient motion states or in the presence of external disturbances.
Since the restoring force from the return system acts on the ball through the push plates, an inherent friction force arises at the contact surface between the push plate and the ball. This friction, if unaddressed, can lead to energy losses, increased wear, and reduced responsiveness of the ball centering mechanism. To optimize system performance and ensure smooth operation, it is critical to minimize this contact friction. To address this, the design incorporates a roller mechanism at the interface between each push plate and the surface of the ball. These miniature rollers, mounted directly on the push plate surface, allow the contact point to roll rather than slide across the spherical surface. This effectively reduces frictional resistance, enhances the responsiveness of the return force, and minimizes mechanical wear. The addition of this roller interface significantly improves the efficiency

and durability of the return system, contributing to the overall stability, precision, and longevity of the BallBot's balancing performance.

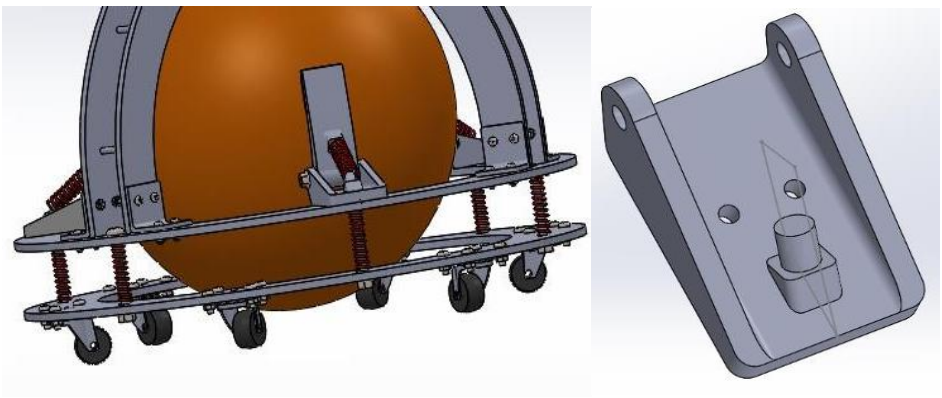

Fig. 7. Ball Return System Design

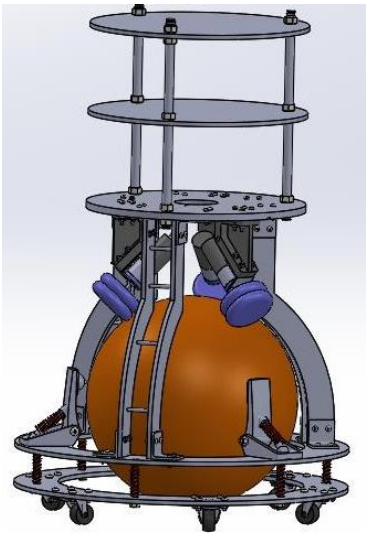

Fig. 8. Robot: The final 3D design of the BallBot

The final 3D design of the BallBot, shown in Figure 8, integrates all major structural and functional components in a compact and modular layout. The robot features a three-level upper frame supported by vertical columns, providing mounting space for control electronics, sensors, and batteries. The core of the robot consists of a spherical balancing ball, driven by three omni-wheel assemblies positioned at 120° intervals and inclined at 45° angles to the base plane. These wheels enable omnidirectional motion and precise control of the robot's orientation. To maintain central alignment of the ball during movement, the design includes a spring-based return mechanism, which incorporates rollers at the ball–push plate interface to reduce friction and improve responsiveness. Additionally, the support platform includes caster wheels for passive rolling and spring-damped mounting bolts to ensure consistent ground contact. This comprehensive mechanical configuration ensures that the BallBot achieves high stability, re-centering accuracy, and adaptability for future control and automation integration.

3. RESULTS AND DISCUSSION

The completed BallBot prototype, as shown in Figure 9, closely follows the finalized 3D design and demonstrates successful translation from digital model to physical assembly. The structure features a three-tier modular frame fabricated from laser-cut MDF sheets, with vertical standoffs ensuring structural rigidity and accessibility. The robot's core balance is maintained using a spherical ball, supported by three omni wheel modules arranged symmetrically around the ball's equator. Each module includes a motorized omni wheel positioned at 45°, driven by a DC motor for omnidirectional control. The upper layers host key electronic components, including a microcontroller, motor driver modules, and a lithium battery pack. The lower base integrates spring-loaded brackets, which stabilize the frame and ensure uniform contact with the ball. The final assembly validates the effectiveness of the mechanical design, modularity for maintenance, and readiness for control algorithm deployment and real-world testing.

Fig. 9. The completed BallBot prototype

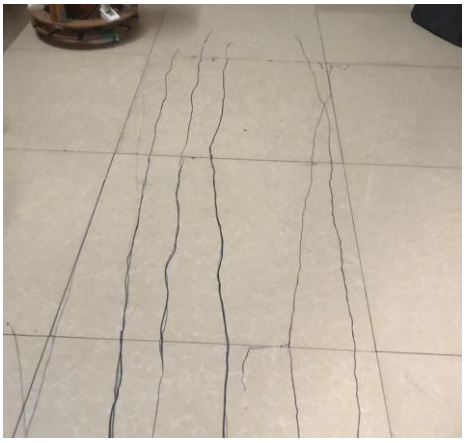

Fig. 10. Trajectory Test: Straight-Line Motion

Figure 10 illustrates the BallBot's trajectory during a test where it was commanded to move forward in a straight line five consecutive times. The resulting paths were marked on the ground to evaluate the robot's directional stability and motion repeatability. While the robot was able to maintain a generally straight trajectory, deviations between the runs are noticeable, with some paths exhibiting lateral drift. These deviations are likely attributed to asymmetrical motor response, wheel slip, ball surface irregularities, or uneven ground contact pressure. Additionally, the passive return system may introduce slight restoring forces that affect directional consistency during low-speed movement. Despite these variations, the robot demonstrated a repeatable tendency to follow forward motion, validating the effectiveness of the omni-wheel drive configuration and structural balance. Further improvements in motor control algorithms, wheel calibration, and PID tuning are expected to enhance linear trajectory precision in future iterations.

The initial design objective of the BallBot was to sustain a load of 50 N while maintaining a stable velocity of 0.5 m/s. Table 1 presents the experimentally measured average velocities for load levels ranging from 0 N to 50 N, tested over five trials per load. The results indicate that while the BallBot was able to achieve the target speed under no load (mean velocity ≈ 0.49 m/s), its performance declined progressively with increasing load. At 10 N, the average velocity dropped to 0.42 m/s, and by 30 N, the system only achieved 0.12 m/s, indicating a 75% reduction from its unloaded performance. Notably, the robot could not move at all under 40 N and 50 N, as reflected by the recorded zero velocities in all trials. These findings suggest that while the system performs reliably under light to moderate loads, its drive torque, traction, or power delivery is insufficient for heavier payloads. This highlights the need for future enhancements in motor torque capacity, power-to-weight ratio, and control optimization to meet the original load-carrying specification.

Table 1. Maximum speed of BallBot when running with load

	No Load	10N	20N	30N	40N	50N
1	0.504	0.4432	0.2215	0.1512	0	0
2	0.496	0.4121	0.2121	0.1132	0	0
3	0.5143	0.4528	0.1514	0.1245	0	0
4	0.4814	0.3842	0.1853	0.0915	0	0
5	0.4524	0.4212	0.1742	0.124	0	0
Average	0.48962	0.4227	0.1889	0.12148	0	0

To evaluate the BallBot's baseline performance on inclined terrain, a series of tests was conducted with no load applied to the robot. As shown in Table 2, five test runs were recorded, yielding velocities ranging from 0.4524 m/s to 0.5143 m/s, with an average of approximately 0.4896 m/s. This result is consistent with the original

design goal of achieving 0.5 m/s under nominal conditions. The BallBot successfully maintained straight-line motion with minimal deviation, demonstrating good balance and effective omni-wheel drive coordination on a sloped surface. These results confirm that, in the absence of external loading, the mechanical design and drive configuration are sufficient to achieve stable and near-target velocity performance, even on inclined terrain.

Table 2. Maximum speed of BallBot when running on an inclined plane without a load

Angle	0	10	20	30
1	0.504	0.4512	0.4412	0.315
2	0.496	0.4224	0.4117	0.3274
3	0.5143	0.4327	0.4578	0.3457
4	0.4814	0.4787	0.4283	0.3164
5	0.4524	0.4601	0.4617	0.2978
Average	0.48962	0.45	0.44014	0.32046

4. CONCLUSIONS

In this study, a complete mechanical design and prototype of a BallBot system were developed, focusing on stability, structural rigidity, and efficient integration of drive and support components. The robot was engineered to move using three omni-wheel modules mounted at 45° angles on a spherical balancing ball. To enhance stability and protect internal components, the design incorporated a robust support frame, a spring-damping platform, and a friction-minimizing ball return system. The spring-loaded components were carefully calculated to ensure mechanical durability, load capacity, and responsiveness.

Experimental results confirmed that the BallBot operates effectively at low payloads and achieves near-target speeds under unloaded and inclined conditions. However, when subjected to loads approaching the design limit of 50 N, the robot exhibited a sharp decline in mobility, with full motion failure observed at 40–50 N. These findings demonstrate that while the system is mechanically stable and modular, its current drive configuration lacks the torque required for high-load operation.

In future work, efforts will focus on improving the robot's actuation system by integrating higher torque motors and optimizing the power-to-weight ratio. Control algorithm refinement, including PID tuning and dynamic feedback adaptation, will be pursued to improve trajectory accuracy and stability under varying load conditions. Additional work will also explore the integration of onboard sensors and closed-loop balancing algorithms, as well as testing in more complex environments to evaluate real-world performance and expand the robot's practical applications.

Author Contributions: Conceptualization, TVM, NXQ; methodology and investigation, NTA, TTT; validation, TTT; writing - original draft preparation, TVM, NXQ, NTA, TTT; writing - review and editing, TTT; All authors have read and agreed to the published version of the manuscript.
Funding: This paper has received no external funding.
Conflicts of interest: There is no conflict of interest.

REFERENCCE

[1] Asgharian, P.; Panchea, A.M.; Ferland, F. (2022), *A Review on the Use of Mobile Service Robots in Elderly Care*. Robotics*, 11,* 127. https://doi.org/10.3390/robotics11060127

[2] Tagliavini, L., Colucci, G., Botta, A. *et al.* (2022), *Wheeled Mobile Robots: State of the Art Overview and Kinematic Comparison Among Three Omnidirectional Locomotion Strategies*. J Intell Robot Syst., 106, 57, https://doi.org/10.1007/s10846-022-01745-7

[3] Dörfler, Kathrin, et al. (2022), *Additive Manufacturing using mobile robots: Opportunities and challenges for building construction*, Cement and concrete research, 158, 106772. https://doi.org/10.1016/j.cemconres.2022.106772

[4] Zhao, Xingwei, et al. (2021), *Accuracy analysis in mobile robot machining of large-scale workpiece*. Robotics and Computer-Integrated Manufacturing, 71, 102153. https://doi.org/10.1016/j.rcim.2021.102153

[5] Tian, Yongding, et al. (2022), *Intelligent robotic systems for structural health monitoring: Applications and future trends*, Automation in construction, 139, 104273. https://doi.org/10.1016/j.autcon.2022.104273

[6] X. Zhao, B. Tao and H. Ding, (2022), *Multimobile Robot Cluster System for Robot Machining of Large-Scale Workpieces*, in IEEE/ASME Transactions on Mechatronics, 27(1), 561-571, doi: 10.1109/TMECH.2021.3068259

[7] Pereira, R.; Carvalho, G.; Garrote, L.; Nunes, U.J. (2022), *Sort and Deep-SORT Based Multi-Object Tracking for Mobile Robotics: Evaluation with New Data Association Metrics*. Appl. Sci., 12, 1319. https://doi.org/10.3390/app12031319

[8] Chakraborty, S.; Elangovan, D.; Govindarajan, P.L.; ELnaggar, M.F.; Alrashed, M.M.; Kamel, S. A (2022), *Comprehensive Review of Path Planning for Agricultural Ground Robots*. Sustainability, 14, 9156. https://doi.org/10.3390/su14159156

[9] D. Ba Pham *et al*., (2023), *Balancing and Tracking Control of Ballbot Mobile Robots Using a Novel Synchronization Controller Along With Online System Identification*, in IEEE Transactions on Industrial Electronics, 70(1), 657-668, 2023, doi: 10.1109/TIE.2022.3146642.

[10] Enemegio, R.; Jurado, F.; Villanueva-Tavira, J. (2024), *Experimental Evaluation of a Takagi–Sugeno Fuzzy Controller for an EV3 Ballbot System*. Appl. Sci., 14, 4103. https://doi.org/10.3390/app14104103

[11] Tham, B. C., Pham, D. B. (2023). *Modeling and second-order sliding mode control for a full three-dimensional ridable ballbot*. International Journal of Modelling and Simulation, 45(3), 948–969. https://doi.org/10.1080/02286203.2023.2246834

[12] Buzzetti, G., Zappetti, D., Iacca, G. (2024). *A Reinforcement Learning Method to Minimize the Damage on a Falling Ballbot*. In: Secchi, C., Marconi, L. (eds) European Robotics Forum 2024. ERF 2024. Springer Proceedings in Advanced Robotics, 32. Springer, Cham. https://doi.org/10.1007/978-3-031-76424-0_15

[13] Enemegio, R.; Jurado, F.; Villanueva-Tavira, J. (2024), *Experimental Evaluation of a Takagi–Sugeno Fuzzy Controller for an EV3 Ballbot System*. Appl. Sci., 14, 4103. https://doi.org/10.3390/app14104103

[14] Fornarelli, L.; Young, J.; McKenna, T.; Koya, E.; Hedley, J. Stastaball, (2023), *Design and Control of a Statically Stable Ball Robot*. Robotics, 12, 34. https://doi.org/10.3390/robotics12020034

[15] Zhou, J., Hu, F., Chong, L. *et al.* (2025), *Robust control of ball-balancing robot using fractional-order PID optimized via particle swarm*. J Braz. Soc. Mech. Sci. Eng. 47, 310, https://doi.org/10.1007/s40430-025-05614-w

[16] Hoang, U.T., Kim, T.D., Le, H.X. *et al.* (2022), *Adaptive Fuzzy Hierarchical Sliding Mode Control for Ball Segway*. Aut. Control Comp. Sci., 519–532, https://doi.org/10.3103/S0146411622060050

[17] Tomar, B., Kumar, N., Sreejeth, M. (2024), *Augmentation in Performance of Real-Time Balancing and Position Tracking Control for 2-DOF Ball Balancer System Using Intelligent Controllers*. Wireless Pers Commun, 138, 2227–2257, https://doi.org/10.1007/s11277-024-11591-5

[18] Fornarelli, L.; Young, J.; McKenna, T.; Koya, E.; Hedley, J. Stastaball: (2023), *Design and Control of a Statically Stable Ball Robot*. Robotics, 12, 34. https://doi.org/10.3390/robotics12020034

[19] Mustary, Shabnom, et al. (2024), *Mathematical model and evaluation of dynamic stability of industrial robot manipulator: Universal robot*. Systems and Soft Computing, 6, 200071, https://doi.org/10.1016/j.sasc.2023.200071

[20] S. Park, (2024), *Design, Implementation, and Control of a Ball-Balancing Robot*, in IEEE Access, 12, 127380-127389, doi: 10.1109/ACCESS.2024.3456238.

Received: September 12th, 2025 / Received in the revised form: December 04th, 2025 / Accepted: December 15th, 2025 / Paper available online: December 20th, 2025